Supplementary Information for "Stability and equilibrium structures of unknown ternary metal oxides explored by machine-learned potentials"

Seungwoo Hwang[1], Jisu Jung[1], Changho Hong[1], Wonseok Jeong[1], Sungwoo Kang[1,], and Seungwu Han[1,2,*]*

[1]Department of Materials Science and Engineering and Research Institute of Advanced Materials, Seoul National University, Seoul 08826, Korea. [2]Korea Institute for Advanced Study, Seoul 02455, Korea.

Validation of the structure relaxation methods

We have validated that the single-shot calculations with SCAN functional on structures relaxed by PBE (PBE/SCAN scheme) yield a reasonable energy accuracy when compared to full relaxation using SCAN functional. Figure S1 illustrates the differences between the energies of structures for the final phases in Figure 2 relaxed using SCAN functional (E_{SCAN}) and those relaxed using PBE functional, followed by single-shot SCAN calculation ($E_{PBE/SCAN}$). Notably, the energy differences of all structures fall within an energy range below 40 meV atom^{-1}. Given that the candidate structure selection process involves an energy window of 50 meV atom^{-1}, these structures would remain in the candidate pool during the evolutionary algorithm, even when the evolutionary algorithm is conducted by machine-learned potentials trained by PBE functional. Furthermore, we have investigated whether the energy orderings of candidate structures change when we apply the PBE/SCAN scheme instead of using SCAN full relaxations. Figure S2 shows this test result for some selected compounds, comparing the energies of the final candidate structures calculated by both PBE/SCAN scheme and SCAN full relaxations. The outcomes reveal that the energy orderings remain largely unaffected when using the PBE/SCAN scheme instead of SCAN full relaxations. These observations therefore validate the PBE/SCAN scheme for energy evaluation at the final stage.

Validation of the negligible magnetic alignment of 4d and 5d transition metals

We have performed the spin-polarized calculations on 40 stable compounds that contain 4d/5d transition metals and found that only Cs_2PtO_3, Rb_2PtO_3, and $OsAlO_4$ exhibit magnetic moments of 0.8, 0.8, and 0.5 Bohr magneton per Pt or Os ion, respectively. We have also examined the

energy orderings of candidate structures of Cs_2PtO_3 and $OsAlO_4$ with and without considering spin polarization (see Figure S3), and our results confirmed that the energy ordering does not significantly change whether the spin polarization is considered or not.

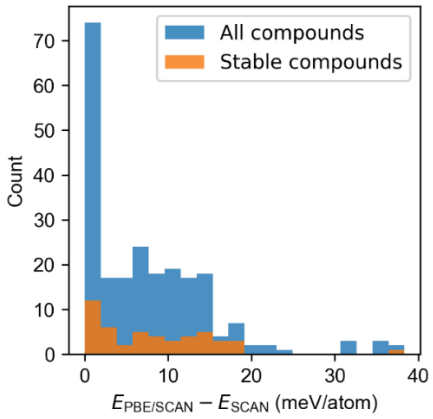

Figure S1. The distribution of energy difference between the structure fully relaxed by SCAN functional (E_{SCAN}), and structure relaxed by PBE followed by single-shot SCAN calculation ($E_{PBE/SCAN}$).

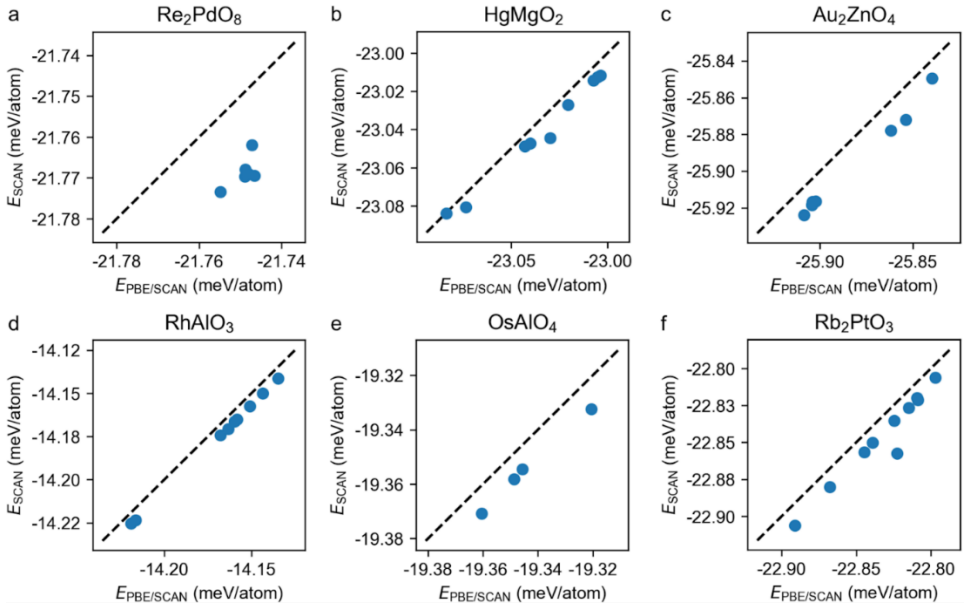

Figure S2. Energy comparison of structures fully relaxed by SCAN functional (E_{SCAN}), versus those relaxed by PBE followed by single-shot SCAN calculation ($E_{PBE/SCAN}$) of (a) Re_2PdO_8, (b) $HgMgO_2$, (c) Au_2ZnO_4, (d) $RhAlO_3$, (e) $OsAlO_4$, and (f) Rb_2PtO_3.

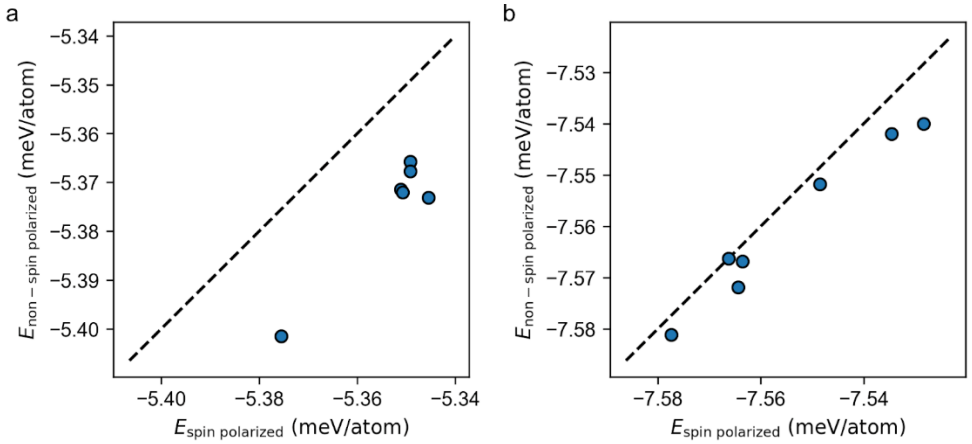

Figure S3. Energy comparison of candidate structures with the composition of (a) Cs_2PtO_3 and (b) $OsAlO_4$, with and without considering spin polarization.

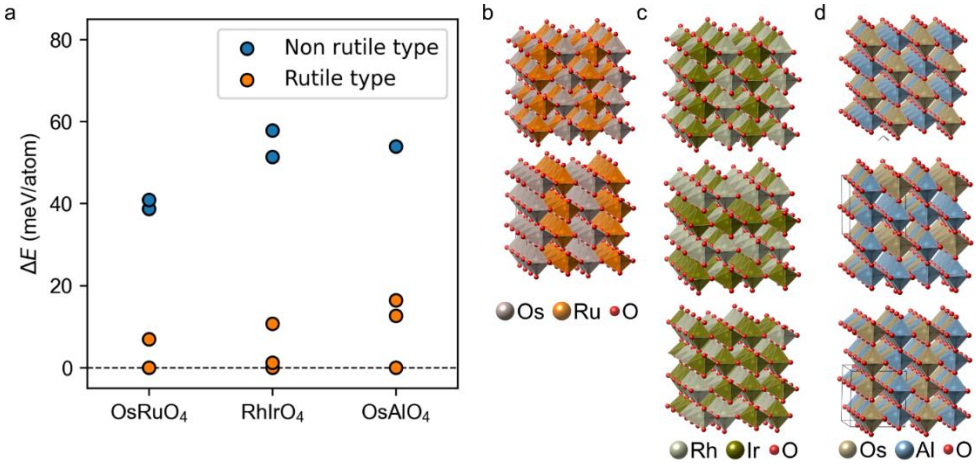

Figure S4. (a) Energy difference between the lowest-energy structure and metastable structures (ΔE) of $OsRuO_4$, $RhIrO_4$, and $OsAlO_4$. Rutile-type structures are marked with orange dots, while other types of structures are marked with blue dots. Atomic structures of candidates with rutile-type structures of (b) $OsRuO_4$, (c) $RhIrO_4$, and (d) $OsAlO_4$.

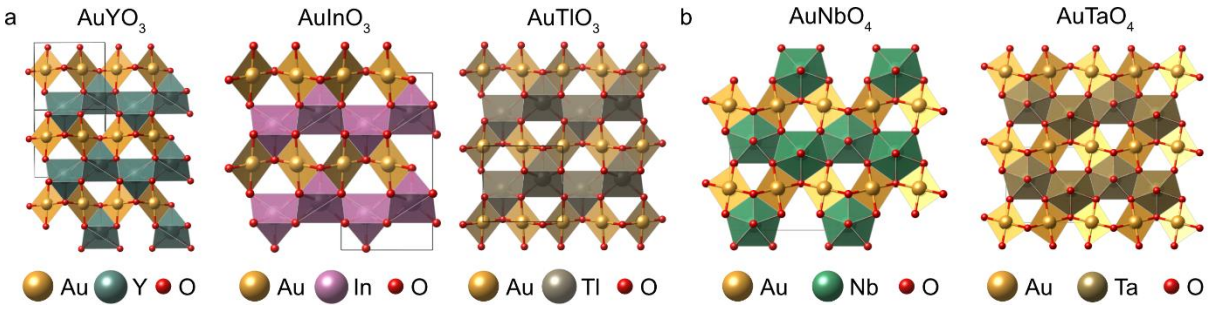

Figure S5. Atomic structures of (a) $AuYO_3$, $AuInO_3$, and $AuTlO_3$, and (b) $AuNbO_4$ and $AuTaO_4$.

Table S1. The table compares the lowest hull energy (E_{hull}) obtained by SPINNER, OQMD,[1] and MP.[2] The hull energies are calculated using the SCAN functional, as described in the main text.[3,4] We also present E_{hull} values evaluated by including hypothetical structures from other databases (marked by †), if they are different from the values evaluted by solely using experimental phases. The unit for E_{hull} is meV atom^{-1}. Compositions written in boldface represent those with the lowest E_{hull} among the structures obtained from SPINNER, OQMD, and MP. The underlined entries under SPINNER indicate that the composition recommended by the recommender system exhibits the lower E_{hull} than that obtained through common oxidation states. Additionally, for the stable structures obtained with SPINNER, corresponding bandgap (E_g) in eV and dielectric constant (ε_0) values are provided. The band gaps are calculated using one-shot hybrid functional calculations, while the dielectric constants are calculated using LDA functional.[5]

SPINNER			OQMD		MP	
Formula	E_{hull}	E_g (ε_0)	Formula	E_{hull}	Formula	E_{hull}
Na_2HfO_3	−273.8/ −101.8†	6.3 (11.3)	**Na_2HfO_3**	−273.8	$Na_2Hf_2O_5$	17.9
Cs_2HfO_3	−241.9/ −78.9†	5.4 (13.5)	**Cs_2HfO_3**	−241.9	**Cs_2HfO_3**	−241.9
Rb_2PtO_3	−209.7/ 23.3†	0 (-)	**Rb_2PtO_2**	−248.9	$RbPtO_3$	261.4
Cs_2PdO_2	−195.5/ −107.3†	1.8 (14.3)	$Cs_2Pd_3O_4$	−147	$CsPdO_3$	362.5
Cs_2PtO_3	−158.2/ −16.2†	0 (-)	**$CsPtO_2$**	−213.1		

Rb_2BeO_2	−115/ −34.5†	3.7 (8.9)	Rb_2BeO_4	361.4	**$Rb_2Be_2O_3$**	−115
$OsRhO_4$	−111.7	0 (-)	$Os_6Rh_4O_9$	263.7		
$CsRhO_2$	−108.5/ −62.9†	0.3 (116.0)	Cs_4RhO_4	−100.9		
$RbRhO_2$	−105.7/ 128.4†	0.3 (25.4)	**$RbRhO_2$**	−234.1	$RbRhO_3$	210.1
$YAuO_3$	−104.1	3.6 (10.8)	$YAuO_2$	15.1	$YAuO_2$	15.5
Au_2CdO_4	−99.7	2.6 (9.8)	$AuCdO_3$	19.6	$AuCdO_2$	−21.5
Cs_2BeO_2	−88.6/ 1.5†	3.8 (9.7)	$Cs_4Be_3O_5$	−80.3	**Cs_2BeO_2**	−90.1
Au_2HgO_4	−86.2	2.0 (13.5)	Au_2HgO_4	54		
$AgAuO_2$	−76.9/ 0.3†	2.4 (14.0)	$AgAu_2O_4$	113.7	**$AgAuO_2$**	−77.2
Au_2PbO_4	−74.7/ −69.7†	1.1 (16.0)	Au_2PbO_4	18.2	$AuPbO_2$	−21.6
$PdMgO_3$	−71.9/ −22.5†	3.1 (10.6)	**Pd_3MgO_6**	−102.1		
$AuTlO_3$	−56.6	1.0 (13.6)	$AuTlO_3$	−1.5	$AuTlO_2$	37.1
$NbAuO_4$	−53.6	3.1 (16.2)	$NbAuO_3$	111.6		
Au_2MgO_4	−53.4	3.0 (7.3)	Au_2MgO_4	39.8	$AuMgO_2$	42.3
Au_2ZnO_4	−47.3	2.3 (11.1)	Au_2ZnO_4	48.5	$AuZnO_3$	1054.2
$OsIrO_4$	−38.6	0 (-)	**$OsIrO_4$**	−38.6		
Re_2BeO_8	−38.5	5.3 (4.7)	Re_2BeO_8	25.2	$ReBeO_3$	1488.5

$TaAuO_4$	−38.2	2.9 (19.9)	$TaAuO_3$	136.6		
$RuPdO_4$	−37.2	0 (-)	$RuPdO_4$	−31.1		
$PdPtO_4$	−34.7	1.2 (30.2)	$PdPtO_4$	−1.2		
Au_2BeO_4	−32.8	2.8 (8.2)	Au_2BeO_4	147	$AuBeO_3$	1049.7
$RhIrO_4$	−27.1/ 6.0†	0 (-)	**$RhIrO_4$**	−33.1		
$PdAu_2O_4$	−27.1	1.4 (12.1)	$PdAu_2O_2$	31.5	$PdAuO_2$	27.5
Y_2HgO_4	−26	3.9 (11.0)	Y_2HgO_4	−18.7	Y_2HgO_4	−18.8
$MgPbO_3$	−25.8	1.8 (12.8)	$MgPbO_3$	136.1	Mg_2PbO_4	116.4
$PdHgO_3$	−25.2/ 22.5†	2.2 (13.5)	**Pd_3HgO_6**	−111.3		
$OsPdO_4$	−25	0 (-)	$OsPdO_3$	204.3		
$RuOsO_4$	−23.6/ 3.3†	0 (-)	**$RuOsO_4$**	−26.9		
Re_2OsO_9	−23.4	0 (-)	$ReOsO_4$	600.3		
$HgTl_2O_2$	−22.8	2.5 (13.3)	$HgTl_2O_4$	31.9	$HgTlO_3$	690
$LaAgO_2$	−16.8/ 30.2†	4.2 (11.5)	**$LaAgO_3$**	−117.6	$LaAgO_2$	−14.2
$MgHgO_2$	−16.4	3.2 (8.8)	**$MgHgO_2$**	−16.4	$MgHgO_3$	779.1
$AuInO_3$	−12.8	2.5 (10.9)	$AuInO_2$	32.5	$AuInO_2$	34.6
$NbRuO_4$	−12.5	0 (-)	$NbRuO_4$	87.6		
$YAgO_2$	−8.8	3.8 (10.3)	**YAgO**	−51.9	$YAgO_2$	−4.9
$OsGaO_4$	−7.8	0 (-)	$OsGaO_4$	44		

$TaReO_6$	−7.4	4.0 (16.2)	$TaReO_4$	308.5	$TaReO_6$	−1
$RhAlO_3$	−4.8	3.8 (10.2)	$RhAlO_4$	97.2	$RhAlO_3$	14.3
$OsAlO_4$	−3.8/ 2.5[†]	0 (-)	**$OsAlO_4$**	−6.3		
Re_2PdO_8	−1.8	2.8 (8.0)	Re_2PdO_8	2.6		
Rb_2MgO_2	0.1		**Rb_2MgO_2**	0.1	**Rb_2MgO_2**	0.1
Sc_2HgO_4	2.9		Sc_2HgO_4	42.4		
$ScAuO_3$	6.3		$ScAuO_2$	28	$ScAuO_2$	28.1
$CaAg_2O_2$	6.5		$CaAg_3O_4$	−51.5	**$CaAg_2O_4$**	−140.4
$RhPtO_4$	7		$RhPtO_4$	7.6	$Rh_2Pt_2O_5$	281.9
$OsInO_4$	7.3		$Os_2In_2O_7$	122.5	$OsInO_3$	566.7
Cs_2BaO_2	8		Cs_2BaO_2	63.6	$Cs_2Ba_2O_3$	27.1
$CdTl_2O_4$	9.6		**$CdTl_2O_4$**	9.6		
Rb_2BaO_2	11.4		$RbBaO_4$	27.2	$RbBaO_3$	842.7
$IrPtO_4$	12.5		$IrPtO_4$	25.4		
WRu_2O_6	14.6		$WRuO_4$	110.1		
Na_2SrO_2	15.1		Na_2SrO_4	67.5	$NaSrO_3$	959.1
NaCsO	15.4		**NaCsO**	12	$NaCsO_3$	1003.4
Ag_2ZnO_2	15.9		$Ag_2Zn_2O_5$	202.5	Ag_2ZnO_4	70.7
$MgTl_2O_4$	18.9		$MgTl_2O_4$	92.5	$MgTlO_3$	714.6
$MoBeO_4$	19.1		**Mo_2BeO_4**	−5		
$RuAlO_4$	19.1		$RuAlO_4$	168.7		

KCsO	20.2	$KCsO_2$	30.5	$KCsO_3$	823.7
$MoOsO_4$	21	$Mo_4Os_6O_9$	435.6		
$HgIn_2O_4$	21.2	**$HgIn_2O_4$**	21.2	**$HgIn_2O_4$**	21.2
$ReGaO_4$	22.4	$ReGa_2O_6$	65.3		
$IrSnO_4$	23	$IrSnO_4$	102.4		
$RhGaO_3$	24	**$RhGaO_3$**	13.4		
Nb_2OsO_7	25.2	$NbOsO_4$	267.9		
Nb_2PdO_6	25.6	$NbPdO_4$	83.5		
$BeZnO_2$	25.7	$BeZnO_2$	41.1	$BeZn_3O_4$	35.3
$ZrAu_2O_5$	25.8	$ZrAuO_2$	566.6		
Li_2BaO_2	28.6	Li_2BaO_4	78.7	Li_4BaO_3	85

Table S2. The table compares the lowest hull energy obtained by SPINNER ($E_{\text{hull}}^{\text{SPINER}}$) and OQMD ($E_{\text{hull}}^{\text{OQMD}}$) for the same compositions. Specifically, it focuses on systems where SPINNER produces a higher hull energy than OQMD when utilizing the scheme in the present study. The compositions listed in the table correspond to those with the lowest hull energy in the OQMD. The unit for E_{hull} is meV atom^{-1}.

Formula	$E_{\text{hull}}^{\text{SPINER}}$	$E_{\text{hull}}^{\text{OQMD}}$
Rb_2PtO_2	−165.9	−248.9
$CsPtO_2$	−249.4	−213.1
Pd_3MgO_6	−102.1	−102.1
Pd_3HgO_6	−111.8	−111.3
$LaAgO_3$	−114.9	−117.6
YAgO	−72.0	−51.9
$CaAg_3O_4$	−51.8	−51.5
Mo_2BeO_4	289.6	−5
$Ir_2Cd_2O_7$	−76.0	−76.1
$ScOs_2O_6$	−3.2	−19.9
$PdAlO_2$	−15.1	−15.5
Os_2MgO_6	−84.4	−84.4
Ir_2MgO_6	−68.2	−67.9
$Ir_2Hg_2O_7$	−49.1	−48.9

(1) Kirklin, S.; Saal, J. E.; Meredig, B.; Thompson, A.; Doak, J. W.; Aykol, M.; Rühl, S.; Wolverton, C. The Open Quantum Materials Database (OQMD): Assessing the Accuracy of DFT Formation Energies. *Npj Comput Mater* 2015, *1* (1), 15010.

(2) Jain, A.; Ong, S. P.; Hautier, G.; Chen, W.; Richards, W. D.; Dacek, S.; Cholia, S.; Gunter, D.; Skinner, D.; Ceder, G.; Persson, K. A. Commentary: The Materials Project: A Materials Genome Approach to Accelerating Materials Innovation. *Apl Mater* 2013, *1* (1), 011002.

(3) Sun, J.; Ruzsinszky, A.; Perdew, J. P. Strongly Constrained and Appropriately Normed Semilocal Density Functional. *Phys Rev Lett* 2015, *115* (3), 036402.

(4) Zhang, Y.; Kitchaev, D. A.; Yang, J.; Chen, T.; Dacek, S. T.; Sarmiento-Pérez, R. A.; Marques, M. A. L.; Peng, H.; Ceder, G.; Perdew, J. P.; Sun, J. Efficient First-Principles Prediction of Solid Stability: Towards Chemical Accuracy. *Npj Comput Mater* 2018, *4* (1), 9.

(5) Youn, Y.; Lee, M.; Hong, C.; Kim, D.; Kim, S.; Jung, J.; Yim, K.; Han, S. AMP2: A Fully Automated Program for Ab Initio Calculations of Crystalline Materials. *Comput Phys Commun* 2020, *256*, 107450.